

Egyptian Journal of Chemistry

http://ejchem.journals.ekb.eg/



Remediation of Lead and Arsenic Ions from Wastewater Using Magnetic Adsorbents

Hoyeda E. Ibrahim¹, Zeinab. M. Anwar¹, Alaa Eldin Y. Ismael¹, Mahmoud O. Abd El-Magied *² ¹ Chemistry Department, Faculty of Science, Suez Canal University, Ismailia 41522, Egypt ² Egypt Department of Isotopes Geology, Nuclear Materials Authority, P.O. Box 530, El Maadi, 11936, Cairo, Egypt



Abstract

This study investigates the remediation of lead and arsenic pollution from wastewater using synthesized and characterized magnetic adsorbents. Magnetite (Fe-Mag), magnetic chitosan (Chito-Fe-Mag), and magnetic magnesium ferrite (Mg-Fer) were synthesized and characterized in the remediation of lead and arsenic ions from water. The remediation of lead ions was optimum at pH 6, at which the Mg-Fer, Fe-Mag, and Chito-Fe-Mag surfaces attract Pb ions via electrostatic and coordination interactions. Conversely, arsenic adsorption was maximized at pH 2.5, where positively charged adsorbent surfaces interacted with arsenic anionic species. The removal efficiencies of both metal ions increased with longer contact time and higher initial concentrations. Maximum lead adsorption capacities were achieved after 90 minutes for Mg-Fer and Fe-Mag and 120 minutes for Chito-Fe-Mag, with corresponding capacities of 109.41, 93.87, and 132.45 mg/g. On the other hand, maximum arsenic adsorption capacities were attained after 120 minutes for all three adsorbents, reaching 26.96, 29.78, and 39.84 mg/g for Mg-Fer, Fe-Mag, and Chito-Fe-Mag, respectively. The initial concentration of lead and arsenic ions may affect the remediation capacity due to its effects on mass transfer resistance and the availability of both free active sites and metal ion ratios. Langmuir, Dubinin-Radushkevich, and pseudo-second-order models show an acceptable fit with experimental data. According to the Langmuir model, the maximum adsorption capacities of Mg-Fer, Fe-Mag, and Chito-Fe-Mag were 129.87, 114.94, and 136.99 mg/g for lead and 34.60, 38.76, and 46.08 mg/g for arsenic, respectively. The mean free energy (E) values suggest that the adsorption processes are primarily physical in nature. The higher adsorption efficiencies achieved (up to 78.3 for As and up to 98.1 for Pb) suggest the potential of these Mg-Fer, Fe-Mag, and Chito-Fe-Mag for wastewater treatment applications.

Keywords: Magnetic adsorbents; Magnetite nanoparticles; Chitosan; Magnesium ferrite; Lead; Arsenic; Remediation.

1. Introduction

The contamination of water bodies with heavy metals has become a prominent environmental issue [1]. Lead (Pb) and arsenic (As) are heavy metal and pose significant risks to human health and aquatic life. Lead is a soft, malleable and bluish-gray metal [2, 3]. Lead does not react with water but reacts with acids (such as hydrochloric acid). Lead forms a protective oxide layer when exposed to air, making it somewhat resistant to corrosion [3]. The lead element primarily occurs in the +2 and +4 oxidation states; however, the +2-oxidation state is the more stable state [2, 3]. Lead is commonly used in lead-acid batteries, radiation shielding applications, paints, and alloys [2]. Lead and its compounds are toxic and accumulate in the body, leading to cumulative poisoning [3, 4]. This toxicity increases with solubility of lead compounds. In children, lead accumulation can cause cognitive deficits, in adults, progressive renal disease. Symptoms include abdominal pain, diarrhea transitioning to constipation, nausea, vomiting, dizziness, headache, and weakness [3]. On the other hand, arsenic (As) is widely distributed in the environment and is known to be highly toxic to humans [5]. Arsenic in the soil environment normally occurs in the +3 and +5 oxidation states [5, 6]. As³⁺ is more toxic and more mobile in soil than As⁵⁺. Arsenic has been suggested to play a biological role in trace amounts. However, high exposures to arsenic in water, sediment, and soil, have proved to be toxic for plants, animals, and humans. Chronic arsenic exposure, mainly through contaminated drinking water, causes diverse health problems, including various cancers, diabetes, neurotoxicity, and skin lesions [7]. Both natural (like erosion and weathering of crustal rocks) and anthropogenic activities (like industrial processes, mining, metallurgy, and industrial and urban waste) release metal ions compounds into the environment [7]. Therefore, the remediation of these metal pollutions from fresh and wastewater sources is essential for minimizi

Conventional methods for heavy metal removal, such as precipitation, coagulation, solvent extraction, distillation, adsorption, and electrochemical methods, have limitations like high cost, sludge generation, and low efficiency for diluted solutions. Adsorption is a surface phenomenon where metal ions (adsorbate) adhere to the surface of a solid material (adsorbent) due to physical or chemical interaction between two phases (adsorbate and adsorbent) [8]. Adsorption is an effective technique that is widely used in water treatment for removing heavy metal from water due to its efficiency, versatility, and relative simplicity [9-13].

*Corresponding author e-mail: mahmoud nma@yahoo.com.; (Mahmoud O. Abd El-Magied). Received Date: 28 June 2025, Revised Date: 27 July 2025, Accepted Date: 24 August 2025 DOI: 10.21608/EJCHEM.2025.398796.11977

In recent years, the development of magnetic adsorbents has presented a promising alternative for heavy metal remediation due to their unique properties, such as high surface area, ease of separation, and reusability [5, 8, 14]. Magnetic adsorbents are materials that combine adsorptive and magnetic properties [15, 16]. The magneto responsive adsorbents benefit from the combination of features inherent to both their components: magnetic beads and adsorbents functional groups. The particles impart magnetic properties to the adsorbents. These properties allow for the rapid and easy separation of adsorbents from the adsorption medium by the application of an external magnetic field without the need of any filtration apparatus [15]. This improves the operative technology of recovery and separation of adsorption process [17]. Therefore, such magnetic adsorbents continue to attract the attention of many investigators [8]. Magnetic adsorbents include magnetic nanoparticles and magnetic polymers (organic and inorganic material) [8, 15, 18, 19]. Magnetic graphene oxide/manganese ferrite adsorbents prepared by coprecipitation method have been used to remove lead and arsenic from water [20]. The remediation lead and arsenic was maximum at pH 5, and 4-6.5, respectively [20]. Magnetic chitosan adsorbent was synthesized for arsenic removal from water [21]. The highest adsorption efficiency for arsenic removal, 20.1 mg/g, was obtained at pH 3. Magnetic chitosan/graphene oxide adsorbent was synthesized for arsenic removal from water [22]. The maximum chitosan/graphene oxide adsorbent capacity, 45 mg/g was obtained at pH 7.3. Arsenic removal from water was studied using magnetic carbon nanocomposites [23]. The results demonstrated that the presence of magnetite particles into the magnetic carbon nanocomposites matrix increases the adsorption of arsenic [24]. Adsorption of lead and arsenic using poly(amidoamine)/carbon nanotubes/silver nanoparticles was studied. Adsorption efficiencies of 76-99 and 76% of Pb(II) and As(III) were attained within 15 min. The removal of Pb(II) and As(III) on the adsorbents was chemisorption process followed the pseudo-second-order and Langmuir models [23]. Another study investigated the adsorption of As(V), Pb(II), Cd(II), and Cr(III) from aqueous solutions using natural and modified chabazite [25]. Natural chabazite exhibited the highest adsorption capacity for Pb(II). Modification enhanced As(V) adsorption by 79%, enabling the modified zeolite to remove both cations and anions from aqueous solutions [25].

This study investigates the remediation of lead and arsenic pollution in wastewater using synthesized and characterized magnetic adsorbents. The magnetic adsorbents will be applied to remove lead and arsenic ions from liquid samples, and the role of factors like metal ion concentration, pH, and contact time on the adsorption process will be evaluated. The influence of each factor will be analyzed to optimize the adsorption process. Further analysis will involve determining the kinetics and isothermal parameters, which characterize the rate and mechanism of lead and arsenic ions from liquid samples by the used magnetic adsorbents.

2. Experimental

2.1. Chemicals

Arsenic and lead standard solutions (1000 mg/L As and Pb, traceable to NIST SRM H₃AsO₄ and Pb(NO₃)₂ in 0.5 mol/L HNO₃, respectively) served as sources of As and Pb ions. Solution acidity was adjusted with diluted NaOH and HCl. Magnetic chitosan adsorbent (Chito-Fe-Mag) was prepared from chitosan extracted from shrimp waste, following the procedure outlined in our previous work [26]. The following Sigma-Aldrich and Merck products were used: magnesium chloride (≥98%), iron(III) hexahydrate (≥98%), iron(III) tetrahydrate (≥98%), zinc chloride (≥98%), sodium hydroxide (≥97%), glacial acetic acid (≥99%), glutaraldehyde (50 wt. % in H₂O), and hydrochloric

2.2. Synthesis of Mg-Fer, Fe-Mag, and Chito-Fe-Mag

Magnetite nanoparticles were prepared using the modified coprecipitation method [15, 27]. Under mechanical stirring, 200 mL of iron (III) chloride solution (2.0 mol/L) was mixed with 200 mL of iron (II) chloride solution (1.2 mol/L), then ammonia solution was added (pH 10-12). After the addition of the ammonia solution, magnetite nanoparticles appeared in the solution. The magnetite nanoparticles (Fe-Mag) were stirred into the solution for 60 min, then were separated, washed with deoxygenated water, and dried at 105°C. Magnetic chitosan adsorbent (Chito-Fe-Mag) was prepared by dissolving 4.0 grams of chitosan in acetic acid solution (120 mL, 6M). The solution was stirred overnight until chitosan solution became homogenous. Under mechanical stirring, the magnetite nanoparticles prepared in the previous step were dispersed in the homogenous chitosan solution. The solution was stirred for 2h, then it was added drop by drop into NaOH/ethanol solution. After the addition of all homogenous chitosan solution into the alkaline solution, the magnetic chitosan beads (chitosan-mag) formed were stirred for additional 24h. The formed beads were separated, washed, and redispersed in glutaraldehyde solution. The mixture was agitated under gentle heating (50°C) for 8h. The product (chitosan-mag/glutaraldehyde or Chito-Fe-Mag) was obtained. The obtained chitosan-mag/glutaraldehyde was washed (ethanol and water) and dried. The magnetic magnesium ferrite (Mg-Fer) was synthesized via the combustion method [28-30]. The stoichiometric concentrations of magnesium and iron chloride salts were dissolved in separate aqueous solutions. The clear magnesium (II) ions solution was added to the clear iron (III) ions solution, under mechanical stirring for 2h. Acetic acid solution was added to the previous solution and stirred for 2h. The pH of the resulting solution was adjusted to pH 8.5. under stirring, the resulting solution was heated to 85 °C. After self-combustion of the obtained acetic/ferrite product, the products obtained were rinsed into water for 2h under stirring. The obtained acetic/ferrite product was dried at 650 °C to remove precursor. After 6h of heating, magnetic magnesium ferrite (Mg-Fer) was obtained.

2.3. Remediation of lead and arsenic ions from water

The remediation of lead and arsenic ions from water was studied using batch experiments. In these experiments several factors were studied and optimized. For solution pH optimizing, several metal ion solutions were prepared. The pH of these solutions was adjusted to different values (1.0-6.5). The magnetic adsorbent particles (0.01 g) were stirred in lead and arsenic solution (0.02 L) for 60 minutes, then recovered and the remaining lead and arsenic concentration were determined using Thermo Elemental Atomic Absorption Spectrometer (SOLAAR S4, England). The adsorption capacity of the Mg-Fer, Fe-Mag, and Chito-Fe-Mag for each metal ions determined using the following Equation (Eq. 1) [15].

$$q_e = \frac{C_i - C_e}{Wt} \times V \quad (1)$$

 $q_e = \frac{C_i - C_e}{Wt} \times V \quad (1)$ where q_e , C_i , C_e , Wt, and V are the adsorption capacity (mg/g) of the Mg-Fer, Fe-Mag, and Chito-Fe-Mag, initial metal ions concentrations (mg/L), remaining (equilibrium) metal ions concentrations (mg/L), weights of Mg-Fer, Fe-Mag, and Chito-Fe-Mag (g) and the volume of metal ions solution (L), respectively. The initial concentration of metal ions in water plays a crucial role in determining the adsorption efficiency and capacity of the adsorbents. To examine how the lead and arsenic initial concentration affects their remediation, several solutions with different lead and arsenic concentration were prepared (24-180 mg/L). The pH of obtained solutions was adjusted to optimum pH from the previous experiments. The magnetic adsorbent particles (0.01 g) were stirred in metal ions solution (0.02 L) for 60 minutes. After equilibrium was attained, the magnetic adsorbent particles were removed from the metal ions solutions, and the remaining lead and arsenic concentration were detected to calculate their remediation capacity to use in adsorption isotherm study. To examine the effect of contact time between lead or arsenic ions and Mg-Fer, Fe-Mag, and Chito-Fe-Mag on the remediation of their ions from water, two solutions of lead and arsenic ions were prepared. The initial concentration of lead and arsenic ions and pH were optimum values from the previous experiments. The magnetic adsorbent particles (0.01 g) were stirred in lead and arsenic ions solution (0.02 L) for different contact times. After that certain period was attained, the magnetic adsorbent particles were removed from the lead and arsenic ions solutions, and the remaining lead and arsenic concentration were detected to calculate their remediation capacity and it in kinetic study. To evaluate the role of solid/liquid ratio on the adsorption process, lead and arsenic ions solutions (pH and initial concentration of lead and arsenic ions were optimum values from the previous experiments) were added to different wights of Mg-Fer, Fe-Mag, and Chito-Fe-Mag particles (0.05-0.16 g). The magnetic adsorbent particles were stirred in lead and arsenic ions solution for optimum contact times evaluated from kinetic study. After equilibrium was attained, the magnetic adsorbent particles were removed from the lead and arsenic ions solutions. The remaining lead and arsenic concentration were detected to calculate their remediation capacity. The efficiency of the used adsorbents (q%) for lead and arsenic ions at different solid/liquid ratio times were determined using Equation 2 [31].

$$q_{\%} = \frac{C_i - C_e}{C_i} \times 100$$
 (2)

3. Results and discussion

3.1. Characterization of the Mg-Fer, Fe-Mag, and Chito-Fe-Mag

Three Mg-Fer, Fe-Mag, and Chito-Fe-Mag adsorbents were prepared, characterized and applied for lead and arsenic remediation studies. The magnetite nanoparticles (Fe-Mag) were prepared using the coprecipitation method, magnetic magnesium ferrite (Mg-Fer) was synthesized via the combustion method, and coated chitosan adsorbent was prepared and then crosslinked with glutaraldehyde to give Chito-Fe-Mag adsorbent. The synthesis of Fe-Mag involves multiple steps including deprotonation, oxidation, and dehydration. Equations 2 represents the Fe-Mag formation.

$$2FeCl3 + FeCl2 + 8NH3 + 4H2O \rightarrow Fe3O4 + 8NH4Cl (3)$$

Magnetic chitosan adsorbent (Chito-Fe-Mag) was prepared from chitosan extracted from shrimp waste, following the procedure outlined in our previous work [26, 32, 33]. The Magnetic chitosan adsorbent was synthesized from the extracted chitosan in a multistep synthesis, Figure 1. In the first step, chitosan extracted from shrimp waste was redissolved in acid media to form a clear chitosan solution. This solution was utilized to coat magnetite nanoparticles by precipitation in alkaline medium. In the second step, the obtained chitosan-mag beads were dispersed in glutaraldehyde solution for crosslinking reaction.

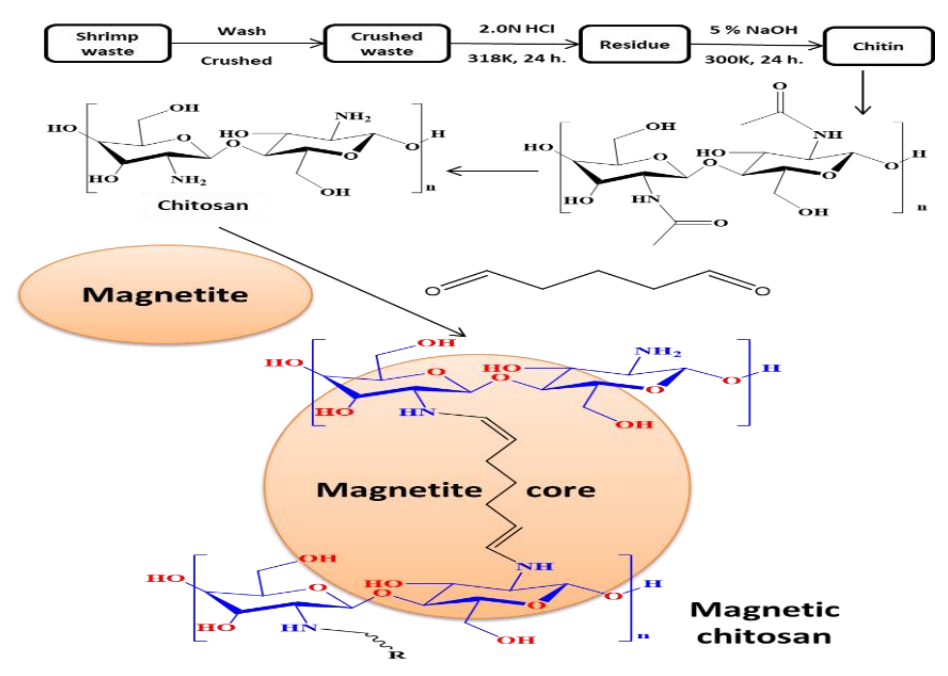


Figure 1 Synthesis of the magnetic chitosan (Chito-Fe-Mag) adsorbent.

The magnetic magnesium ferrite (Mg-Fer) was synthesized via the combustion method [28, 29]. The stoichiometric concentrations of magnesium and iron chloride were mixed and added to acetic acid solution. With heating, a gel type material (acetic/Mg-Fer) is formed and then self-combusted and heated to at 650 °C to produce Mg-Fer, Figure 2.

Three Mg-Fer, Fe-Mag, and Chito-Fe-Mag were characterized prior to their application in remediation of lead and arsenic ions from liquid solutions. FT-IR spectroscopy was used to confirm the presence of characteristic functional groups and the metal-oxygen bonding within the synthesized Mg-Fer, Fe-Mag, and Chito-Fe-Mag, Figure 3. The FT-IR spectrum of the synthesized magnesium ferrite nanoparticles (Mg-Fer) exhibited absorption bands falling within the interval of 420-784 cm⁻¹, which are indicative of spinel ferrite structures (Figure 3(a)). A strong band around 578 cm⁻¹ corresponds to the intrinsic stretching vibrations of the Fe-O bond in the tetrahedral sites, while a weaker band near 420 cm⁻¹ is ascribed to the M-O (Mg-O) vibrations in the octahedral sites [30, 34]. The detection of these absorption bands confirms the achieved formation of the spinel-type structure of Mg-Fe₂O₄) [29, 35]. The synthesis of magnetite was confirmed by FTIR, as depicted in Figure 3(b). The spectrum confirms the existence of Fe-O stretching vibrations at 553 cm⁻¹. In Chito-Fe-Mag, additional bands were detected at 3374-3441 and 1400 cm⁻¹ (O-H and N-H stretching), 1659 and 1727 cm⁻¹ (amine, amide, and CO), and 1068 and 1125 cm⁻¹ (C-O stretching), confirming the achieved coating of magnetite with chitosan, Figure 3(c). These bands indicated the detection of hydroxyl and amine groups responsible for adsorption activity of the (Chito-Fe-Mag) adsorbent.

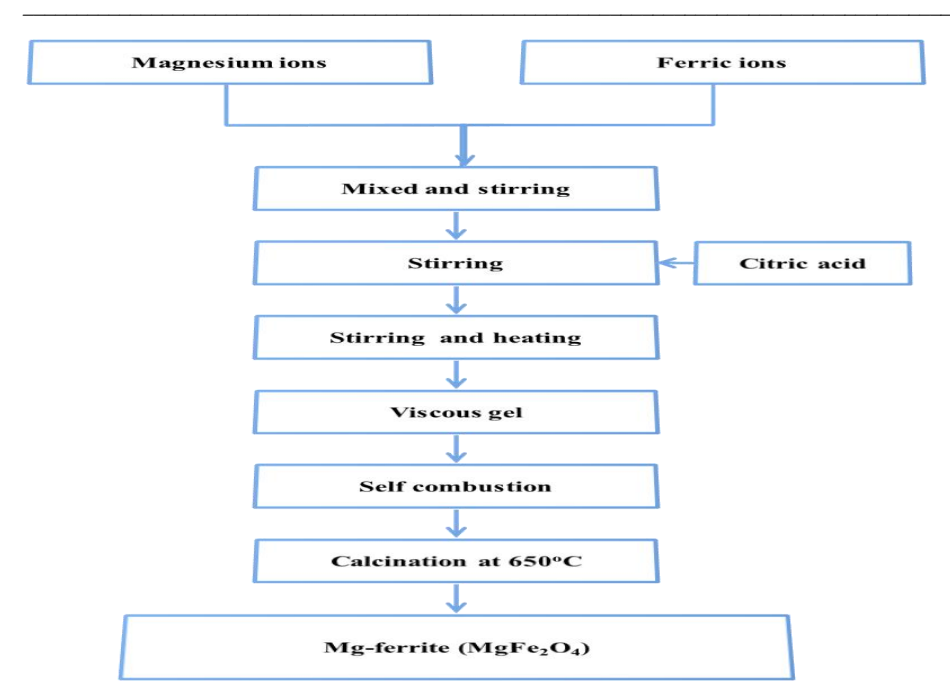


Figure 2 Synthesis of magnetic magnesium ferrite (Mg-Fer) adsorbent.

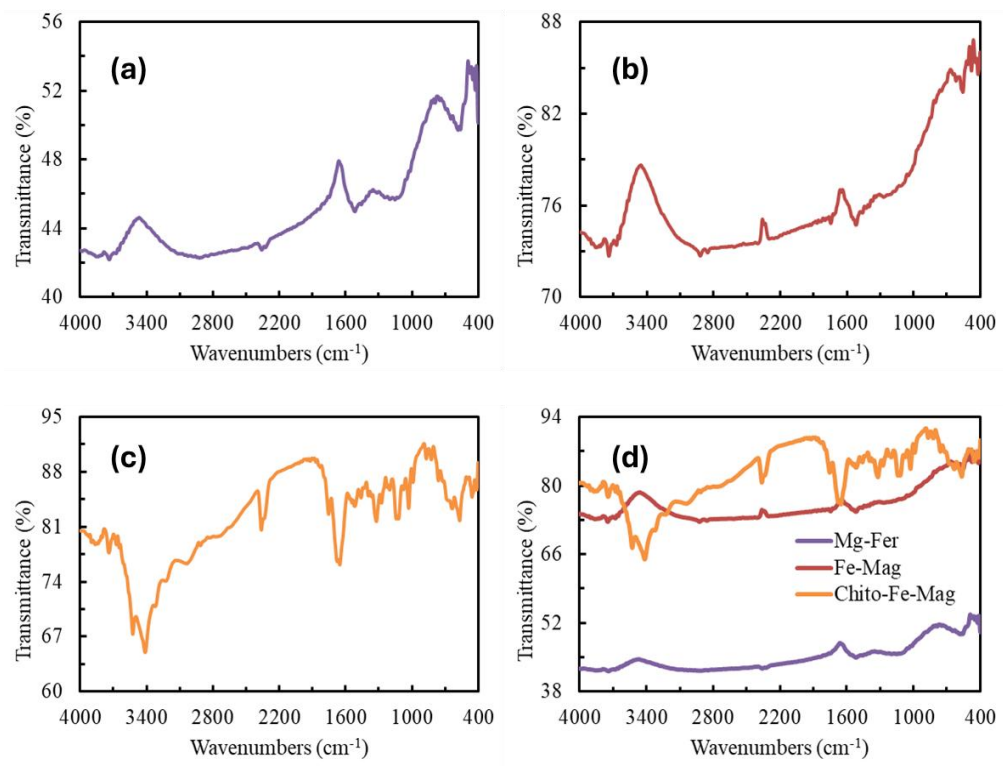


Figure 3 FTIR spectra of Mg-Fer (a), Fe-Mag (b), Chito-Fe-Mag (c), and the three adsorbents combined (d).

SEM images of Mg-Fer, Fe-Mag, and Chito-Fe-Mag showed a difference in morphological structures for the three materials due to their different composition, Figure 4(a-c). Also, the morphological differences between Fe-Mag Chito-Fe-Mag may be due to chitosan encapsulation [36]. The Chito-Fe-Mag surface appeared smoother and more compact, consistent with a chitosan coating. EDX charts of Mg-Fer, Fe-Mag, and Chito-Fe-Mag confirmed the elemental composition of the samples Figure 4(d-e). Magnetite and magnesium ferrite showed strong signals for Fe and O, and Mg in the latter. Magnetic chitosan displayed additional peaks for C and N, corroborating the organic content of chitosan. The elemental ratios were in good agreement with theoretical values, confirming achieved doping and coating processes. X-ray Diffraction (XRD) analysis confirmed the spinel structure of magnetite (Fe-Mag, Fe₃O₄), magnetic chitosan (Chito-Fe-Mag), and magnesium ferrite (Mg-Fer, MgFe₂O₄) nanoparticles. Dynamic Light Scattering (DLS) analysis was conducted to determine the hydrodynamic size distribution and colloidal stability of Mg-Fer, Fe-Mag, and Chito-Fe-Mag materials. DLS analysis revealed distinct size differences and dispersion characteristics of Mg-Fer, Fe-Mag, and Chito-Fe-Mag. The Fe-Mag exhibited a moderate size falling within the interval of 43.8 to

190.1 nm (average size of 116.9 nm), indicating some degree of particle agglomeration possibly due to magnetic interactions. Mg-Fer showed the smallest size (21.4 to 105.7) with an average of 63.7 nm. The smaller average hydrodynamic diameter of Mg-Fer suggests an improved dispersion and reduced aggregation, possibly due to weaker interparticle magnetic forces or better crystallinity. The Chito-Fe-Mag exhibited the largest size (141.8 to 1990 nm with an average size of 779.2 nm). The largest size of Chito-Fe-Mag and greater variation in particle size can be ascribed to the detection of the chitosan polymer coating around the Fe-Mag core. This chitosan layer increases the hydrodynamic radius and can lead to greater variation in particle size. Therefore, the chitosan coating significantly altered the nanoparticles size and dispersity. The increase in hydrodynamic diameter reflects both the physical thickness of the chitosan layer and potential swelling of the polymer in water.

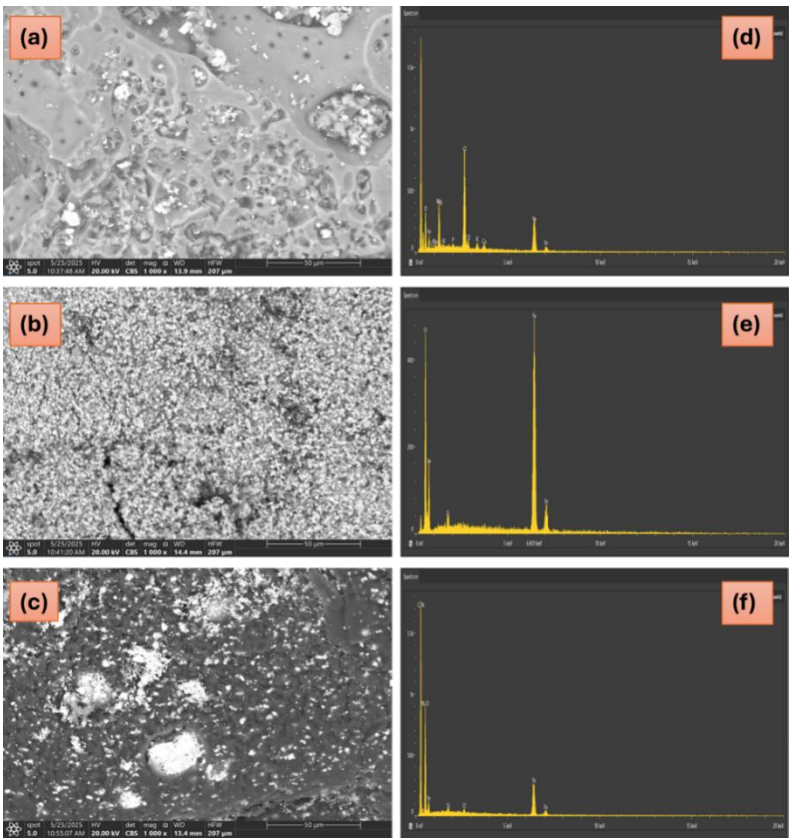


Figure 4 SEM images of Mg-Fer (a), Fe-Mag (b), Chito-Fe-Mag (c), and EDX charts of Mg-Fer (d), Fe-Mag (e), Chito-Fe-Mag (f).

3.2. Effect of pH on the remediation of lead and arsenic

Medium pH significantly influences metal ions adsorption depending on the adsorbent's surface chemistry, the metal speciation, and the other adsorbates competition between H* in the system and metal ions for adsorption sites. The effect of pH on the remediation of lead (50 mg/L) and arsenic (50 mg/L) ions was studied spanning from 1 to 6.5 pH values. The capacities at different pH values, calculated using Eq. 1, were illustrated in Figures 5 (a) and 5(b). The remediation of lead ions was optimum at pH 6, whereas the remediation of arsenic ions was optimum pH 2.5. The used Mg-Fer, Fe-Mag, and Chito-Fe-Mag adsorbents have different functional groups. The functional groups of Mg-Fer and Fe-Mag in water are -OH groups, whereas Chito-Fe-Mag has -NH, -NH2, and -OH groups. For lead remediation: At low pH (pH<3), -NH, -NH2, and -OH groups are protonated, making the Mg-Fer, Fe-Mag, and Chito-Fe-Mag surfaces positively charged. Therefore, Mg-Fer, Fe-Mag, and Chito-Fe-Mag surfaces repel Pb ions and reduce their adsorption capacity. Also, the competition between Pb ions and excess H* ions (H* ions protonate the magnetic adsorbent surface) in the adsorption system for adsorption sites reduce their adsorption capacity. At pH (pH 3-6), the deprotonation of -NH, -NH2, and -OH groups occur, making the Mg-Fer, Fe-Mag, and Chito-Fe-Mag surfaces negatively charged. Therefore, the Mg-Fer, Fe-Mag, and Chito-Fe-Mag surfaces attract Pb ions via electrostatic and coordination interactions. Therefore, this deprotonation increases adsorption capacity. Also, the competition between excess Pb ions and H* ions in the adsorption system vanished at higher pH values. The optimum capacity of Mg-Fer, Fe-Mag, and Chito-Fe-Mag for lead ions (pH 6.0, 60 min., and 0.01g of magnetic adsorbent, and 50 mg/L of lead ions) were 76.41, 52.48, and 92.37 mg/g, respectively. At higher pH (pH>6), lead ions hydrolyzed and precipitated. Several hydroxide species may form like Pb(OH)⁺, Pb(OH)₂, and Pb(OH)₂. Pb(OH)⁺, Figure 5(c) [37], may be adsorbed but with lower affinity due to its large size compared with Pb2+ ions, thus, the adsorption amount decreased. On the other hand, both arsenic forms (+3 and +5 forms) form anionic species (H₂AsO₃⁻, HAsO₃²-, AsO₃³-, H₂AsO₄⁻, HAsO₄²-, AsO₄³-) in aqueous mediums, Figure 5 (d) [7, 38]. As mentioned previously, -NH, -NH₂, and -OH groups are protonated at low pH (pH<3), making Mg-Fer, Fe-Mag, and Chito-Fe-Mag surfaces positively charged. Therefore, the Mg-Fer, Fe-Mag, and Chito-Fe-Mag surfaces attack the negatively charged anionic species of arsenic ions and increases their adsorption capacity [39]. Also, there is no competition between anionic species of arsenic ions and H* for adsorption sites. The optimum capacity of Mg-Fer, Fe-Mag, and Chito-Fe-Mag for arsenic ions (pH 2.5, 60 min., and 0.01g of magnetic adsorbent, and 50 mg/L of arsenic ions) were 19.2, 19.8, 29.6 mg/g, respectively. At higher pH (pH> 2.5), arsenic form anionic species in aqueous mediums where the protonation of -NH, -NH2, and -OH groups increase, making the Mg-Fer, Fe-Mag, and Chito-Fe-Mag surfaces negatively charged. Thus, the arsenic sorption species decreases due to electrostatic repulsions between negatively charged magnetic adsorbent surface and anionic species. Therefore, lead adsorption is facilitated by electrostatic and coordination interactions between the adsorbent surfaces and Pb ions where arsenic adsorption is facilitated by electrostatic interactions. The surface charge properties of nanomaterials critically influence their colloidal stability, adsorption efficiency, and interactions with charged species in aqueous systems. The zeta potential and point of zero charge (PZC) of Mg-Fer, Fe-Mag, and Chito-Fe-Mag were studied. Zeta potential is a key indicator of surface charge and electrostatic stability of colloidal particles. All Mg-Fer, Fe-Mag, and Chito-Fe-Mag exhibited positive zeta potential at pH 2, indicating positively charged surfaces in acidic media. However, at pH 8 all materials exhibited negative zeta potentials, indicating negatively charged surfaces under neutral conditions. Magnesium ferrite displayed a more negative value, suggesting enhanced surface deprotonation or substitutional effects of doped magnesium ions increasing surface acidity. All Mg-Fer, Fe-Mag, and Chito-Fe-Mag showed a positive zeta potential at pH 2.5, ascribed to protonated NH and OH groups on their structure. This positive surface charge enhances its interaction with negatively charged arsenic species. Also, the capacity of Chito-Fe-Mag is higher than that of Mg-Fer and Fe-Mag due to its increased protonated NH and OH function groups. Also, Chito-Fe-Mag tends to agglomerate less in acidic conditions due to repulsive forces among positively charged particles.

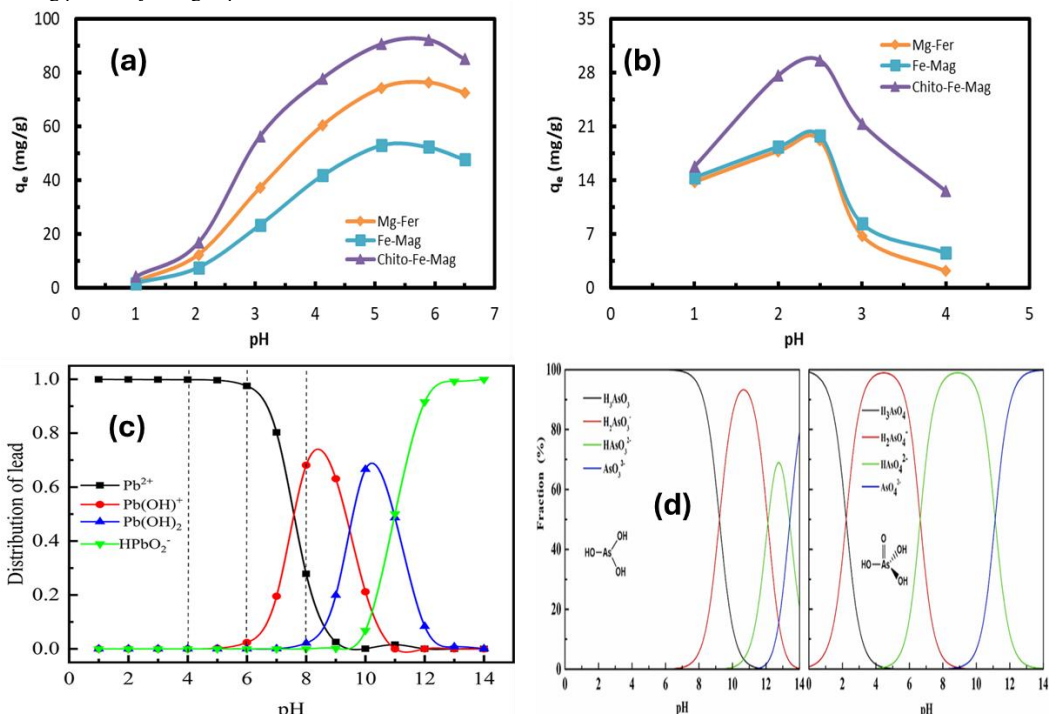


Figure 5 Effect of pH on the remediation of lead (a), arsenic (b), lead species distribution (c), and arsenic (III and V) species distribution (d)

3.3. Effect of initial concentration on the lead and arsenic remediation

The effect of initial concentration of metal ions on the remediation of lead (at pH 6.0) and arsenic (at pH 2.5) ions was studied in the concentration range of 24 to 180 mg/L. The Mg-Fer, Fe-Mag, and Chito-Fe-Mag particles were stirred in metal ions solutions till equilibriums, and then separated, and the lead and arsenic equilibrium concentration were detected to calculate their adsorption capacity. Figures 6(a) and 6(b) show the capacities obtained at different lead and arsenic concentration. The remediation of both metal ions increases as their initial concentration increases. The optimum capacity of Mg-Fer, Fe-Mag, and Chito-Fe-Mag for arsenic and lead ions was obtained at initial concentration of 100 and 140 mg/L of arsenic and lead ions, respectively. The optimum capacity of Mg-Fer, Fe-Mag, and Chito-Fe-Mag for lead ions was 104.27, 84.71, and 120.19 mg/g, respectively. The optimum capacity of Mg-Fer, Fe-Mag, and Chito-Fe-Mag for arsenic ions was 23.27, 25.25, and 32.84 mg/g, respectively. The lead and arsenic concentration may affect the remediation capacity and efficiency of these ions due to resistance to mass transfer and availability of both free active sites and metal ions. As initial concentration of lead and arsenic ions, their ratio to available active sites increases, therefore adsorption capacity increases. Also, higher lead and arsenic initial concentration increase the gradient of mass transfer and therefore enhance adsorption capacity.

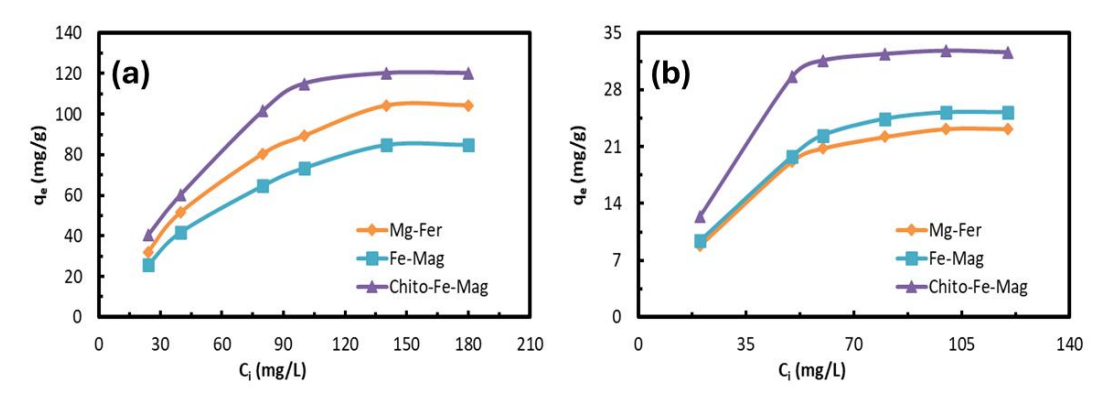


Figure 6 Effects of initial concentration on remediation of lead (a) and arsenic (b) ions from water.

3.4. Adsorption isotherms models

The adsorption isotherms are relationships show the amount of lead and arsenic that can be adsorbed by the Mg-Fer. Fe-Mag, and Chito-Fe-Mag adsorbents (adsorption capacity, qe) in relation to the equilibrium lead and arsenic concentration in lead and arsenic liquid phase (equilibrium concentration, Ce). Adsorption isotherm parameters provide information about the interaction mechanism that occurs between the Mg-Fer, Fe-Mag, and Chito-Fe-Mag adsorbents and the lead and arsenic including adsorption nature, binding constant, adsorption energy, and adsorption affinity. There are several monolayer and multilayer adsorption isotherms used in adsorption of lead and arsenic from water [1]. Langmuir isotherm is a chemical adsorption isotherm models consider the monolayer adsorption process that the adsorbate molecules are adsorbed (Mg-Fer, Fe-Mag, and Chito-Fe-Mag adsorbents) in the adsorption sites of the adsorbents [40]. Langmuir isotherm suggests that the adsorbents (Mg-Fer, Fe-Mag, and Chito-Fe-Mag) and the adsorbate (lead and arsenic) are in dynamic equilibrium (at equilibrium the adsorption rate equals the desorption rate), and the extent of surface coverage (θ) depends on the concentration of the adsorbate. Langmuir isotherm also suggests adsorption in monolayer coverage, all adsorption sites are energetically equivalent, and each adsorption site can hold only one adsorbate molecule, and the ability of a molecule to adsorb in each adsorption site is independent of the occupation of neighboring. The following Equation (Eq. 4) shows the linear form of Langmuir model [1, 41].

$$\frac{C_e}{q_e} = \frac{C_e}{Q_m} + \frac{1}{K_L Q_m} \quad (4)$$

 $\frac{C_e}{q_e} = \frac{C_e}{Q_m} + \frac{1}{K_L Q_m} \end{(4)}$ where Q_m and K_L are the maximum Mg-Fer, Fe-Mag, and Chito-Fe-Mag capacity derived from Langmuir model (mg/g) and ratio of the adsorption rate and desorption rate (L/mg). The Langmuir model can be linearized by plotting C_e/q_e versus C_e values. The equilibrium data were analyzed using Langmuir model. Figures 7(a) and 7(b) show Langmuir plots for the lead arsenic remediation. C_e/q_e versus C_e give straight with high coefficient of determination (R2) values. Therefore, Langmuir isotherm may be used to fit the lead and arsenic remediation using Mg-Fer, Fe-Mag, and Chito-Fe-Mag adsorbents. Table 1 illustrates the values of the maximum Mg-Fer, Fe-Mag, and Chito-Fe-Mag capacity derived from Langmuir model compared to the experimental ones. There is a similarity between the two values, which confirms the suggestion of using Langmuir isotherm to fit the remediation of lead and arsenic ions from water using Mg-Fer, Fe-Mag, and Chito-Fe-Mag adsorbents. The maximum Mg-Fer, Fe-Mag, and Chito-Fe-Mag capacity derived from Langmuir model for lead ions adsorption are 129.87, 114.94, and 136.99 mg/g, respectively. Where the maximum Mg-Fer, Fe-Mag, and Chito-Fe-Mag capacity derived from Langmuir model for arsenic ions adsorption are 34.60, 38.76, 46.08 mg/g, respectively. Based on the Langmuir assumption, fractional coverage (0, the ratio of occupied to total adsorption sites) represents the extent of monolayer surface coverage [40]. The θ value is proportional to the initial lead and arsenic concentrations. Equation S1 (Supplementary File) can be used to determine θ at varying initial concentrations of lead and arsenic [42]. Figures 7(c) and (d) show the fractional coverage (θ) for lead and arsenic at varying initial concentrations. Higher θ values on Mg-Fer, Fe-Mag, and Chito-Fe-Mag surfaces indicate their strong affinity for lead and arsenic remediation. The separation factor (R_L), derived from Langmuir parameters, indicates adsorption favorability: $R_L > 1$ (unfavorable), $R_L = 1$ (linear), and $R_L < 1$ (favorable) [40]. Equation S2 (Supplementary File) can be used to calculate R_L values for the remediation of lead and arsenic ions from water using Mg-Fer, Fe-Mag, and Chito-Fe-Mag adsorbents [43]. Separation factors (R₁) values calculated for lead remediation (0.0509-0.5927) and arsenic remediation (0.1867-0.6765) using Mg-Fer, Fe-Mag, and Chito-Fe-Mag adsorbents were less than 1 (Figures S1 and S2, Supplementary File).

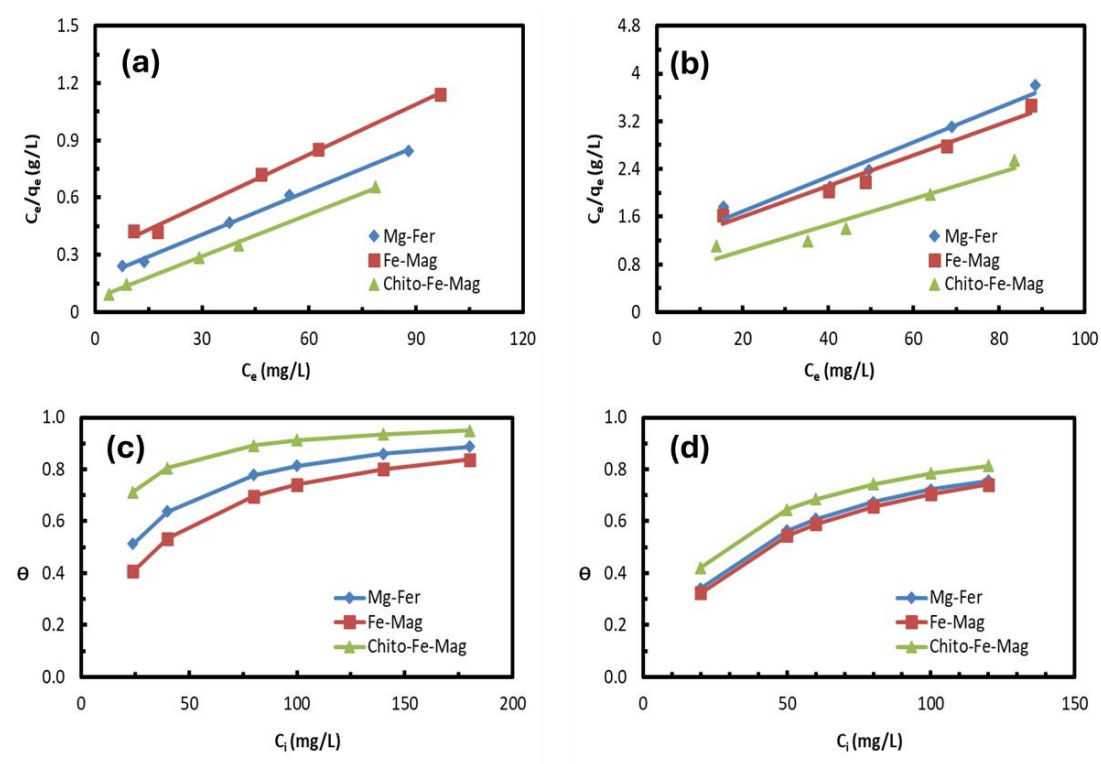


Figure 7 Langmuir model for lead (a) and arsenic (b) remediation, fractional coverage (θ) of lead (c), and fractional coverage (θ) of arsenic

TO 11 4 T		1' ' C1 1		
Table I I anomilir	parameters for the re	emediation of lead	l and argenic	ions from water

Metal ions	Adsorbent	q _e (mg/g)	Q _m (mg/g)	K _L (L/mg)	\mathbb{R}^2
Lead	Mg-ferrite	104.27	129.87	0.0438	0.9976
	Fe-Mag	84.71	114.94	0.0286	0.9942
	Chito-Fe-Mag	120.19	136.99	0.1037	0.9976
Arsenic	Mg-ferrite	23.27	34.60	0.0259	0.9549
	Fe-Mag	25.25	38.76	0.0239	0.96260
	Chito-Fe-Mag	32.84	46.08	0.0363	0.91850

The Freundlich model, an empirical adsorption isotherm, describes multilayer adsorption. Equation 5 presents a Freundlich linear form [44].

$$\log q_e = \frac{\log C_e}{n} + \log K_F \quad (5)$$

 $\log q_e = \frac{\log C_e}{n} + \log K_F \quad (5)$ The Freundlich model's constants, n (heterogeneity) and K_F (adsorption capacity, mg/g), were evaluated for lead and arsenic remediation using equation 5. Figures S3 and S4 (Supplementary File) display the Freundlich isotherm fits (log qe vs. log Ce) for Mg-Fer, Fe-Mag, and Chito-Fe-Mag adsorbents. Values for n and K_F were derived from the slope (1/n) and intercept (log K_F) of these plots. Table 2 compares the Freundlich-derived maximum adsorption capacities with experimental values. Although the log qe vs. log Ce plots exhibited high R² values, the observed n > 1 (Table 2) indicates that the Freundlich isotherm is less acceptable to describe lead and arsenic remediation

Table 2 Freundlich parameters for the remediation of lead and arsenic ions from water

Metal ions	Adsorbent	q _e (mg/g)	K_F (mg/g)	n	\mathbb{R}^2
Lead	Mg-ferrite	104.27	20.51	2.12	0.9665
	Fe-Mag	84.71	8.19	1.900	0.9629
	Chito-Fe-Mag	120.19	8.38	1.50	0.9402
Arsenic	Mg-ferrite	23.27	1.98	1.74	0.9167
	Fe-Mag	25.25	2.03	1.69	0.9378
	Chito-Fe-Mag	32.84	2.075	0.99	0.8958

The Dubinin-Radushkevich (D-R) model is a semi-empirical adsorption model based on Polanyi's potential theory, and it can be used in the modeling of the adsorption processes on porous adsorbents [40, 45]. The D-R model suggests that adsorbent size is comparable to the micropore size, and the adsorption of adsorbates on porous adsorbent materials can be expressed using the adsorption potential (ϵ , ϵ = $RTln(1+1/C_e)$). Here R is the gas constant (8.314 J/mol K), T is the temperature (K), and C_e is the equilibrium concentration of metal ions (mmol/L). The linear form of the D-R model is given by Equation 6 [40].

$$lnq_e = lnQ_{DR} - K_{DR}\varepsilon^2$$
 (6)

Ce and QDR, KDR, and ε represent the equilibrium concentration of metal ions (mmol/L) and the maximum Mg-Fer, Fe-Mag, and Chito-Fe-Mag capacity derived from D-R model (mmol/g), the D-R binding constant (mol²/kJ), the adsorption potential based on the Polanyi's potential theory (kJ/mol), respectively [45]. The calculated K_{DR} values were then used to determine the mean free energy. The mean free energy of remediation of lead and arsenic ions from water using Mg-Fer, Fe-Mag, and Chito-Fe-Mag adsorbents can be calculated using Equation S3 (Supplementary File). E and KDR are the mean free energy of remediation reaction (kJ/mol) and the D-R binding constant (mol²/kJ), respectively. The values of mean free energy are determined to detect the nature of the adsorption processes. Physical adsorption processes have E values less than 8 kJ/mol and chemical adsorption processes have E values more than 8 kJ/mol [40, 45]. The experimental data of lead and arsenic ions remediation was analyzed using Equation 6. Figures 8(a) and 8(b) show D-R plots (In qe versus ε²) for lead and arsenic ions remediation by Mg-Fer, Fe-Mag, and Chito-Fe-Mag adsorbents. The Q_{DR} and K_{DR} values were determined from slope (- K_{DR}) and intercept (ln Q_{DR}) of the ln q_e versus ε² lines. Table 3 illustrates the values of Q_{DR}, K_{DR}, and E derived from D-R model. The D-R model gives straight lines with high R² values and maximum Mg-Fer, Fe-Mag, and Chito-Fe-Mag capacity comparable to the experimental ones. This indicates the favorability of the D-R model to fit the remediation of lead and arsenic ions from water using these adsorbents. The values of E for the lead remediation by the Mg-Fer, Fe-Mag, and Chito-Fe-Mag are falling within the interval of 5.00 to 7.07 kJ/mol. The values of E for the remediation of lead and arsenic remediations using Mg-Fer, Fe-Mag, and Chito-Fe-Mag are in the range of the physical adsorption processes.

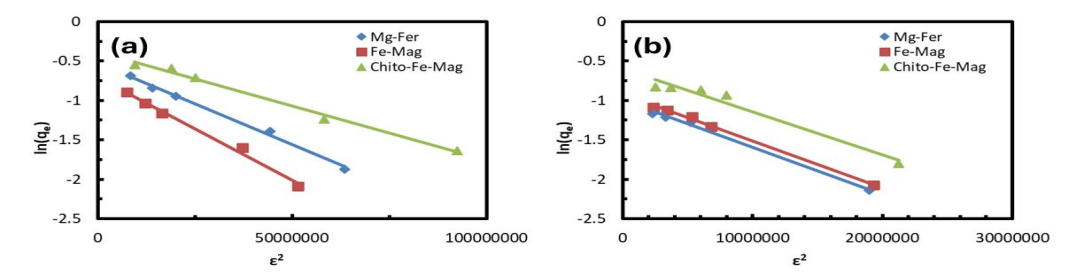


Figure 8 D-R model for remediation of lead (a) and arsenic (b) ions from water.

	1						
Metal ions	Adsorbent	q _e (mg/g)	Q _{DR} (mmol/g)	Q _{DR} (mg/g)	K_{DR} (mol ² /kJ ²)	E (kJ/mol)	R ²
Lead	Mg-ferrite	104.27	0.59	122.62	2.00E-08	5.00	0.9953
	Fe-Mag	84.71	0.49	101.95	2.00E-08	5.00	0.9909
	Chito-Fe-Mag	120.19	0.69	141.95	1.00E-08	7.071	0.9925
Arsenic	Mg-ferrite	23.27	0.37	27.55	6.00E-08	2.89	0.9936
	Fe-Mag	25.25	0.40	29.77	6.00E-08	2.89	0.9974
	Chito-Fe-Mag	32.84	0.55	41.20	5.00E-08	3.16	0.9624

Table 3 Dubinin–Radushkevich parameters for the remediation of lead and arsenic ions from water.

3.5. Effect of time

The contact time between the adsorbent and metal ions in adsorption systems significantly influences the adsorption efficiency. Hence, it is crucial to study the effect of contact time between the lead and arsenic ions and adsorbents to balance efficiency and operational cost. The adsorption capacity of the Mg-Fer, Fe-Mag, and Chito-Fe-Mag for lead and arsenic ions at different contact times was determined and plotted graphically (Figures 9(a) and 9(b)). The results show that the contact time between the Mg-Fer, Fe-Mag, and Chito-Fe-Mag adsorbents and lead or arsenic ions strongly influences the adsorption capacity. The remediation of both metal ions increases as their contact time with the Mg-Fer, Fe-Mag, and Chito-Fe-Mag increases until equilibrium is attained. The optimum capacity of lead ions was obtained after 90, 90, and 120 minutes of contact with Mg-Fer, Fe-Mag, and Chito-Fe-Mag adsorbents, respectively. The optimum capacity of Mg-Fer, Fe-Mag, and Chito-Fe-Mag for lead ions was 109.41, 93.87, and 132.45 mg/g, respectively. On the other hand, the optimum capacity of arsenic ions was obtained after 120 minutes of contact with the adsorbents. The optimum capacity of Mg-Fer, Fe-Mag, and Chito-Fe-Mag for arsenic ions was 26.96, 29.78, and 39.84 mg/g, respectively. The effect of contact time between the Mg-Fer, Fe-Mag, and Chito-Fe-Mag adsorbents and lead or arsenic ions may be divided into three kinetic steps. The initial kinetic step is fast adsorption of lead or arsenic ions on the Mg-Fer, Fe-Mag, and Chito-Fe-Mag adsorbents surfaces due to the availability of all active sites for lead or arsenic ion adsorption. The second kinetic step shows an intermediate adsorption rate for both lead and arsenic adsorption by the Mg-Fer, Fe-Mag, and Chito-Fe-Mag adsorbents. This slowdown in adsorption rate for both lead and arsenic may be due to reduced availability of adsorption sites for lead or arsenic ion adsorption. Also, after the initial rapid adsorption on the Mg-Fer, Fe-Mag, and Chito-Fe-Mag ' surface, adsorption may occur into the Mg-Fer, Fe-Mag, and Chito-Fe-Mag' pores, which is slower than surface adsorption due to possible pore diffusion limitations. The final kinetic step is reaching equilibrium, at which all active sites are occupied with lead or arsenic ions, and according to the Langmuir model, dynamic equilibrium is obtained where the rate of adsorption equals the rate of desorption.

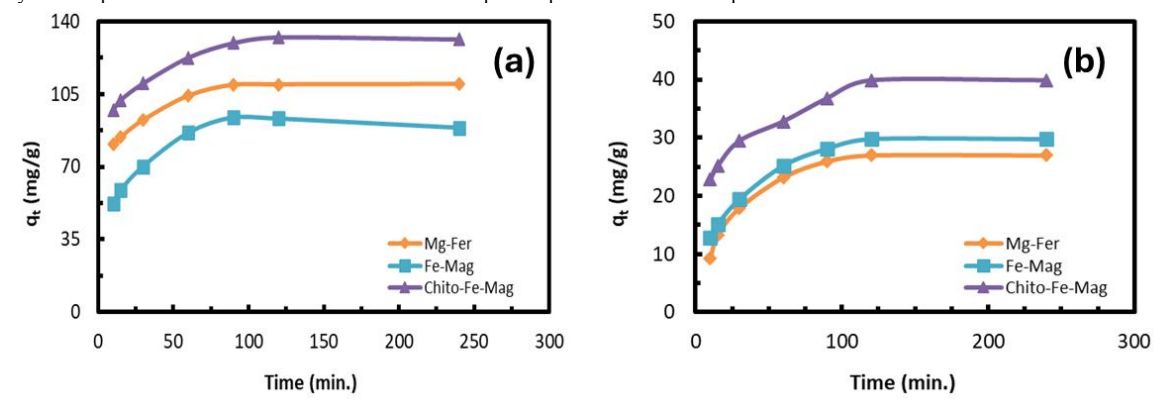


Figure 9 Effect of time on the remediation of lead (a) and arsenic (b) ions from water.

3.6. Adsorption Kinetic models

The pseudo-first order kinetic model is widely used to describe the initial adsorption rate of metal ions onto solid adsorbents. This model is particularly useful for reactions where one of the reactants is present in large excess and does not change significantly during the reaction. Pseudo-first-order kinetic model is particularly useful when one reactant is in significant excess, such as the solvent (water) in single-adsorbate systems, and its concentration does not change significantly during the adsorption reaction. This allows the reaction rate to be effectively determined by the concentration of only one reactant term. The model is represented by Equation 7 [26, 39].

$$\log (q_e - q_t) = \log (Q_1) - \frac{k_1}{2.303}t (7)$$

Where: q_e is the equilibrium adsorption capacity (mg/g); q_t is the adsorption capacity at time t (mg/g); Q_1 is the theoretical adsorption capacity from the pseudo-first order model (mg/g); k_1 is the pseudo-first order rate constant (1/min); and t is the contact time (min). According to the pseudo-first order model, the plot of $\log (q_e - q_t)$ vs. (t) should give a straight line with slop $(-k_1/2.303)$ and intercept $\log(Q_1)$, as illustrated in Figures S5 and S6 (Supplementary File). The values of k1 and Q_1 were determined from slope $(-k_1/2.303)$ and intercept $(\log(Q_1), \text{ respectively})$. The low regression (R^2) values for the lead and arsenic adsorption plots indicate the pseudo-first order model's poor fit to the adsorption data.

Table 4 Pseudo-first-order model parameters for the remediation of lead and arsenic ions from water.

Metal ions	Adsorbent	qe (mg/g)	Q ₁ (mg/g)	k ₁ (min ⁻¹)	R ²
Lead	Mg-ferrite	109.41	42.37	0.0343	0.9916
	Fe-Mag	93.87	58.88	0.0343	0.9935
	Chito-Fe-Mag	132.45	51.39	0.0309	0.9834
Arsenic	Mg-ferrite	26.96	24.97	0.0343	0.9909
	Fe-Mag	29.78	23.34	0.0288	0.9958
	Chito-Fe-Mag	39.84	20.45	0.0203	0.9818

The pseudo-second-order kinetic model is commonly used to describe adsorption processes, often providing a better fit for metal ion adsorption systems than the pseudo-first-order model. The model is represented by Equation (8) [26, 39].

$$\frac{t}{q_t} = \frac{1}{k_2 Q_2^2} + \frac{1}{Q_2} t \quad (8)$$

 $\frac{t}{q_t} = \frac{1}{k_2Q_2^2} + \frac{1}{Q_2}t \quad (8)$ The theoretical adsorption capacity derived from pseudo-second order kinetic model (q₂, mg/g) and pseudo-second order rate constant (k₂, g/mg.min) were determined from the slope (1/Q₂) and intercept (1/k₂.Q₂²) of the log(t/q_t) vs. (t) plots (Figures 10(a) and 10(b)). Generally, the goodness of the kinetic equations may be checked from the consistency of the values of experimental adsorption capacity (q_e) with the value of theoretical adsorption capacity derived from to the used model. As depicted in Table 5, the theoretical (derived from to the pseudo-second order kinetic model) and experimental adsorption capacities were similar. Furthermore, the higher R² value for the pseudosecond order kinetic model in lead and arsenic adsorption indicates its effectiveness in describing the experimental data. These findings suggest that lead and arsenic adsorption is a chemisorption process followed by the pseudo-second order.

Table 5 Pseudo-second-order model parameters for the remediation of lead and arsenic ions from water.

Metal ions	Adsorbent	q _e (mg/g)	$Q_2 (mg/g)$	k ₂ (g/mg.min)	R ²
Lead	Mg-ferrite	109.41	114.94	0.0015	0.9987
	Fe-Mag	93.87	105.26	0.0008	0.9968
	Chito-Fe-Mag	132.45	136.99	0.0013	0.9991
Arsenic	Mg-ferrite	26.96	32.47	0.0013	0.9991
	Fe-Mag	29.78	34.36	0.0015	0.9975
	Chito-Fe-Mag	39.84	42.37	0.0020	0.9931

Generally, metal ion diffusion into porous adsorbents involves both boundary layer diffusion (film diffusion) and intraparticle diffusion. The Weber-Morris model (Equation 9), which examines the relationship between adsorption capacity (q1) and the square root of time (t^{0.5}), is key to determining if pore diffusion limits the adsorption rate [16, 46].

$$q_t = k_{IPD} t^{1/2} + C (9)$$

The intraparticle diffusion rate constant (k_{IPD}, g/mg.min^{0.5}) was determined from the slopes of (q_t) vs. (t^{0.5}) plots (Figures 10(c) and 10(d)). The intercept (C) of these plots relates to film diffusion and boundary layer thickness. The linearity of the intraparticle diffusion plots, with high R2 values, suggests that intraparticle diffusion significantly influences the adsorption of lead and arsenic ions within the magnetic adsorbent pores. Therefore, the intraparticle diffusion is the rate-determining step in the current adsorption process.

Table 6 Intraparticle diffusion model parameters for the remediation of lead and arsenic ions from water.

Metal ions	Adsorbent	q _e (mg/g)	С	k _{IPD} (mg/g min ^{0.5})	\mathbb{R}^2
Lead	Mg-ferrite	109.41	0.3217	0.0224	0.9921
	Fe-Mag	93.87	0.1587	0.032	0.9905
	Chito-Fe-Mag	132.45	0.4063	0.0224	0.9832
Arsenic	Mg-ferrite	26.96	0.0561	0.0299	0.9508
	Fe-Mag	29.78	0.0891	0.0297	0.9809
	Chito-Fe-Mag	39.84	0.2249	0.0281	0.9914

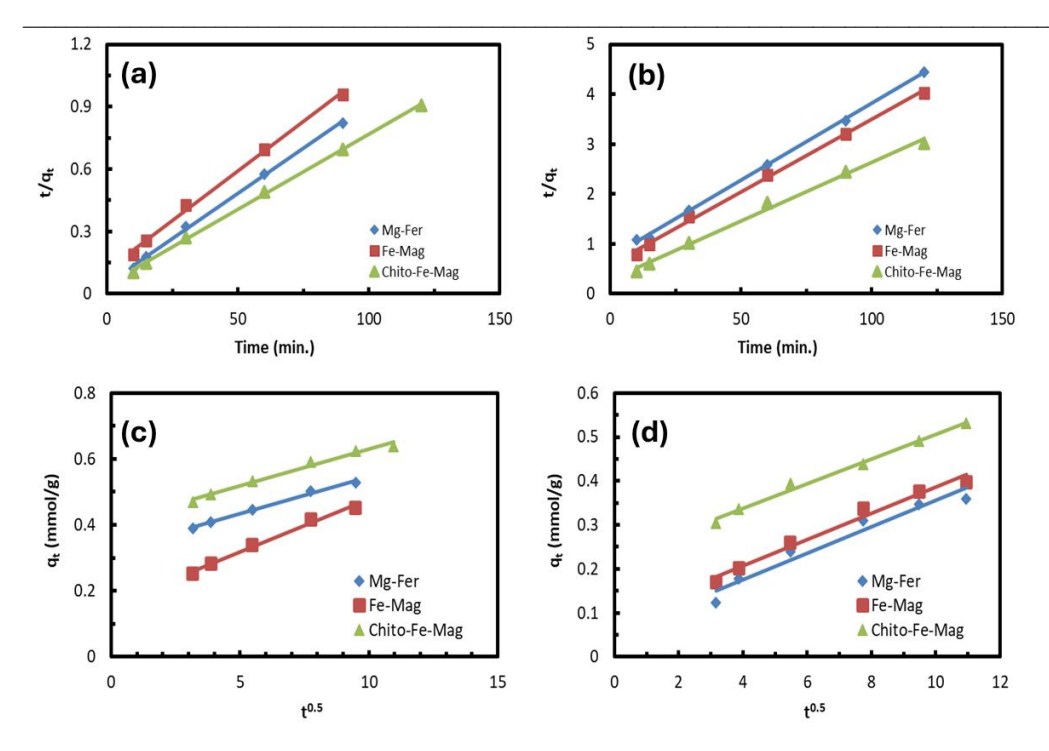


Figure 10 Pseudo-second-order model for lead (a) and arsenic (b) remediation, and intraparticle diffusion model for the remediation of lead (c) and arsenic (d) ions from water.

3.2.4. Effect of adsorbent mass

The solid/liquid ratio represents the amount of magnetic adsorbent (adsorbent mass) relative to the volume of the metal ions solution. The solid/liquid ratio is a key factor affecting the kinetics, efficiency, capacity, and cost of removing metal ions from water using solid adsorbents. This study investigates the effect of the magnetic adsorbent/solution ratio on lead and arsenic remediation. Varying masses of magnetic adsorbent were added to 20 mL of lead and arsenic solutions at optimal pH and initial concentration, and the resulting adsorption efficiency and capacity were evaluated. The results show that low adsorbent masses resulted in lower removal efficiency due to insufficient binding sites on the magnetic adsorbent for lead and arsenic concentrations. Conversely, higher adsorbent masses provide more active sites and surface areas for lead and arsenic ions adsorption, enhancing lead and arsenic ion adsorption and increasing removal efficiency (Figures 11(a) and 11(b)). On the other hand, adsorption capacity shows an inverse relationship with magnetic adsorbent mass. The adsorption capacity decreases with increasing magnetic adsorbent mass. At lower masses, a higher metal ion concentration per gram of adsorbent leads to increased capacity but incomplete removal. As magnetic adsorbent mass increases, the resulting lower metal ion concentration per gram reduces adsorption capacity (Figures 11(c) and 11(d)).

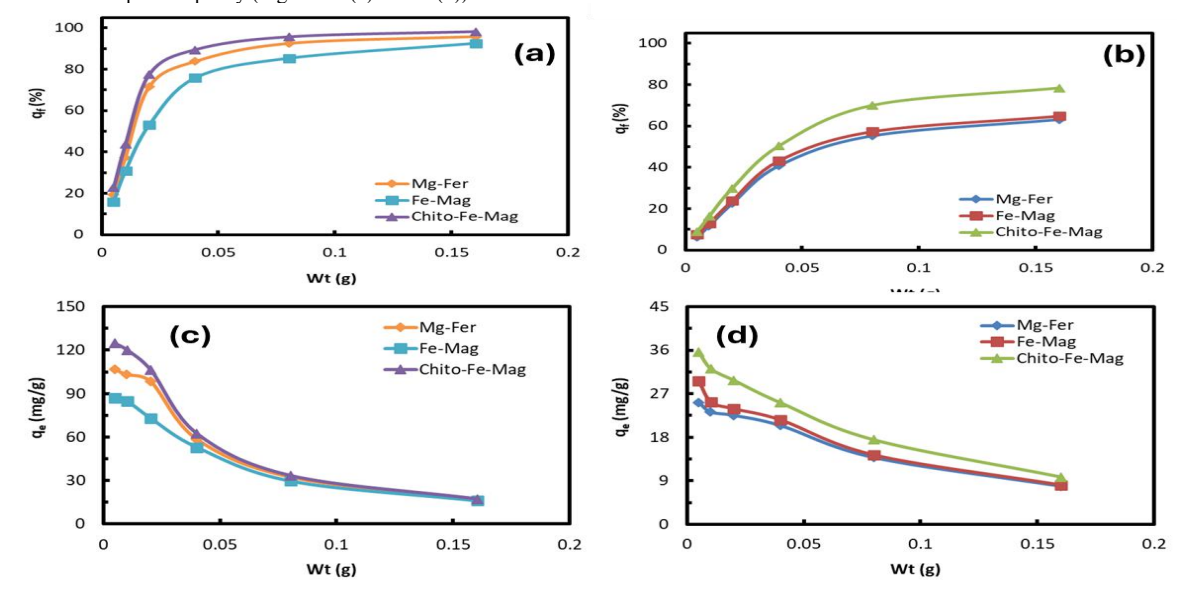


Figure 11 Effects of adsorbent mass on adsorption capacity (mg/g) of lead (a) and arsenic (b) remediation, and adsorption efficiency (%) of lead (c) and arsenic (d) remediation.

5. Conclusions

In this study, three magnetic adsorbents were prepared (Mg-Fer, Fe-Mag, and Chito-Fe-Mag), characterized and applied for heavy metal removal from aqueous solutions. The magnetite nanoparticles (Fe-Mag) were prepared using the coprecipitation method, magnetic magnesium ferrite (Mg-Fer) was synthesized via the combustion method, and magnetic chitosan was prepared and then crosslinked with glutaraldehyde. To give Chito-Fe-Mag adsorbent. The characterization analyses confirmed the structural, size, and functionalization of the adsorbents. XRD confirmed the crystal structure and crystallite size, which were supported by SEM morphology and EDX elemental composition. FTIR provided evidence of surface functional groups, especially in Chito-Fe-Mag. The remediation of lead and arsenic ions from water using these adsorbents was studied using batch experiments. In these experiments several factors were studied and optimized. The optimum conditions were pH 6, 140 mg/L, and 90-120 min of contact time for lead adsorption and pH 6, 100 mg/L, and 120 min of contact time for arsenic adsorption on the used adsorbents. As initial concentration of lead and arsenic ions increases, their ratio to available active sites increases, therefore adsorption capacity increases. Also, higher initial concentration of lead and arsenic ions increases the gradient of mass transfer and enhances adsorption capacity. The experimental data fit Langmuir and Dubinin-Radushkevich isotherm models. The D-R model yielded maximum adsorption capacities for lead on Mg-Fer, Fe-Mag, and Chito-Fe-Mag of 122.62, 101.95, and 141.95 mg/g, respectively, and for arsenic of 27.55, 29.77, and 41.20 mg/g, respectively. The pseudo-second order kinetic model effectively described the adsorption process, as indicated by high R² values and agreement between theoretical and experimental adsorption capacities. Furthermore, the linearity of intraparticle diffusion plots with high R² values suggested that intraparticle diffusion significantly influenced adsorption rates and was likely the rate-determining step. This study supports SDG by offering an economical and environmentally friendly method for heavy metal removal from wastewater.

Declarations

Funding

No funds, grants, or other support was received.

Competing interests

The authors have no relevant financial or non-financial interests to disclose.

References

- [1] J. Yang, B. Hou, J. Wang, B. Tian, J. Bi, N. Wang, X. Li, X. Huang, Nanomaterials for the removal of heavy metals from wastewater, Nanomaterials, 9 (2019) 424. DOI: 10.3390/nano9030424
- [2] A.M. Ghazi, J.R. Millette, 4 Lead, in: R.D. Morrison, B.L. Murphy (Eds.) Environmental Forensics, Academic Press, Burlington, 1964, pp. 55-79. DOI: 10.1016/B978-012507751-4/50026-4
- [3] A. Carocci, A. Catalano, G. Lauria, M.S. Sinicropi, G. Genchi, Lead toxicity, antioxidant defense and environment, in: P. de Voogt, F.A. Gunther (Eds.) Reviews of Environmental Contamination and Toxicology, vol 238, Springer International Publishing, Cham, 2016, pp. 45-67. DOI:10.1007/398 2015 5003
- [4] M.O. Oromaiwele, D.E. Odiase, Azanza garckeana extract alleviates lead-induced testicular toxicity: A Histological and Oxidative Stress Analysis, Fertility & Reproduction, 07 (2025) 43-47. DOI: 10.1142/s2661318225500021
- [5] Q. Lu, K. Choi, J.-D. Nam, H.J. Choi, Magnetic polymer composite particles: design and magnetorheology, Polymers, 13 (2021) 512. DOI: 10.3390/polym13040512
- [6] J.O. Nriagu, P. Bhattacharya, A.B. Mukherjee, J. Bundschuh, R. Zevenhoven, R.H. Loeppert, Arsenic in soil and groundwater: an overview, in: Trace Metals and other Contaminants in the Environment, Elsevier, 2007, pp. 3-60. DOI: 10.1016/S1875-1121(06)09001-8
- [7] M.M. Chaudhary, S. Hussain, C. Du, B.R. Conway, M.U. Ghori, Arsenic in water: understanding the chemistry, health implications, quantification and removal strategies, ChemEngineering, 8 (2024) 78. DOI: 10.3390/chemengineering8040078
- [8] D. Mehta, S. Mazumdar, S.K. Singh, Magnetic adsorbents for the treatment of water/wastewater—A review, Journal of Water Process Engineering, 7 (2015) 244-265. DOI: 10.1016/j.jwpe.2015.07.001
- [9] L.A. Yousef, A.R. Bakry, M.O. Abd El-Magied, Uranium(VI) recovery from its leach liquor using zirconium molybdophosphate composite: kinetic, equilibrium and thermodynamic studies, Journal of Radioanalytical and Nuclear Chemistry, 323 (2019) 549-556. DOI: 10.1007/s10967-019-06871-5
- [10] I. Abdelfattah, W. Abdelwahab, A. El-Shamy, Montmorillonitic clay as a cost effective, eco friendly and sustainable adsorbent for physicochemical treatment of contaminated water, Egyptian Journal of Chemistry, 65 (2022) 687-694. DOI: 10.21608/ejchem.2021.92320.4378
- [11] H.M. Al-Saidi, A.A. Gahlan, O.A. Farghaly, Decontamination of zinc, lead and nickel from aqueous media by untreated and chemically treated sugarcane bagasse: a comparative study, Egyptian Journal of Chemistry, 65 (2022) 715-724. DOI: 10.21608/ejchem.2021.79170.3882
- [12] W. Thabet, S.B. Ahmed, o. Abdelwahab, N.F. Soliman, Enhancement adsorption of lead and cadmium ions from waste solutions using chemically modified palmfibers, Egyptian Journal of Chemistry, 63 (2020) 4917-4927. DOI: 10.21608/ejchem.2020.31220.2663
- [13] Y.W. Al-Bizreh, E. Hamada, M. AL-Joubbeh, New adsorbent from red beet roots (CRBR) for removal of lead, Egyptian Journal of Chemistry, 62 (2019) 513-524. DOI: 10.21608/ejchem.2018.3904.1342
- [14] A.S. Mahmoud, N. Youssef, A.M. Osama, M. Selim, Removal of lead ions from industrial wastewater using magnetite loaded on silica support, Egyptian Journal of Chemistry, 62 (2019) 2163-2173. DOI: 10.21608/ejchem.2019.5807.1499
- [15] A.M. Donia, A.A. Atia, E.M.M. Moussa, A.M. El-Sherif, M.O. Abd El-Magied, Removal of uranium(VI) from aqueous solutions using glycidyl methacrylate chelating resins, Hydrometallurgy, 95 (2009) 183-189. DOI: 10.1016/j.hydromet.2008.05.037
- [16] M.O. Abd El-Magied, M.M. Rezk, Y.I. Bakr, M.M. Fawzy, M. Sopaih, Z.M. Anwar, Removal of uranium ions from contaminated solutions by adsorption on cerium and lanthanum magnesium ferrite, Journal of Radioanalytical and Nuclear Chemistry, 334 (2024) 1049-1066. DOI: 10.1007/s10967-024-09889-6
- [17] T.L. da Silva, T.B. da Costa, H.S.d.C. Neves, M.G.C. da Silva, M.G.A. Vieira, Methods of Synthesis of Magnetic Adsorbents, in: L. Meili, G.L. Dotto (Eds.) Advanced magnetic adsorbents for water treatment: fundamentals and new perspectives, Environmental Chemistry for a Sustainable World, vol 61. Springer International Publishing, Cham, 2021, pp. 25-58. DOI: 10.1007/978-3-030-64092-7_2

Egypt. J. Chem. 69, No. 2 (2026)

- [18] M.O. Abd El-Magied, A.A. Tolba, H.S. El-Gendy, S.A. Zaki, A.A. Atia, Studies on the recovery of Th(IV) ions from nitric acid solutions using amino-magnetic glycidyl methacrylate resins and application to granite leach liquors, Hydrometallurgy, 169 (2017) 89-98. DOI: 10.1016/j.hydromet.2016.12.011
- [19] M.O. Abd El-Magied, Sorption of uranium ions from their aqueous solution by resins containing nanomagnetite particles, Journal of Engineering, 2016 (2016) 1-11. DOI: 10.1155/2016/7214348
- [20] S. Kumar, R.R. Nair, P.B. Pillai, S.N. Gupta, M.A.R. Iyengar, A.K. Sood, Graphene oxide–MnFe2O4 magnetic nanohybrids for efficient removal of lead and arsenic from water, ACS Applied Materials & Interfaces, 6 (2014) 17426-17436. DOI: 10.1021/am504826q
- [21] Z. Jiang, N. Li, P.-Y. Li, B. Liu, H.-J. Lai, T. Jin, One-step preparation of chitosan-based magnetic adsorbent and its application to the adsorption of inorganic arsenic in water, Molecules, 26 (2021) 1785. DOI: 10.3390/molecules26061785
- [22] A.I.A. Sherlala, A.A.A. Raman, M.M. Bello, A. Buthiyappan, Adsorption of arsenic using chitosan magnetic graphene oxide nanocomposite, Journal of Environmental Management, 246 (2019) 547-556. DOI: 10.1016/j.jenvman.2019.05.117
- [23] G.M. Neelgund, S.F. Aguilar, M.D. Kurkuri, D.F. Rodrigues, R.L. Ray, Elevated adsorption of lead and arsenic over silver nanoparticles deposited on poly(amidoamine) grafted carbon nanotubes, Nanomaterials, 12 (2022) 3852. DOI: 10.3390/nano12213852
- [24] A.A. Burbano, V.L. Lassalle, M.F. Horst, G. Gascó, A. Méndez, The effect of carbon coating on the arsenite sorption by magnetic carbon nanocomposites, International Journal of Environmental Science and Technology, 22 (2025) 4749-4760. DOI: 10.1007/s13762-024-05924-x
- [25] L.A. Pinedo-Torres, A. Bonilla-Petriciolet, M.E. García-Arreola, Y. Villagrana-Pacheco, A.G. Castañeda-Miranda, M.S. Berber-Mendoza, J.A. Cecilia, Adsorption of arsenic, lead, cadmium, and chromium ions from aqueous solution using a protonated chabazite: preparation, characterization, and removal mechanism, Adsorption Science & Technology, 2023 (2023) 2018121. DOI: 10.1155/2023/2018121
- [26] M.O. Abd El-Magied, High-efficiency recovery of cerium ions from monazite leach liquor by polyamines and polycarboxylates chitosan sorbents prepared from marine industrial wastes, Int J Biol Macromol, 243 (2023) 125243. DOI: 10.1016/j.ijbiomac.2023.125243
- [27] Y.-k. Sun, M. Ma, Y. Zhang, N. Gu, Synthesis of nanometer-size maghemite particles from magnetite, Colloids and Surfaces A: Physicochemical and Engineering Aspects, 245 (2004) 15-19. DOI: 10.1016/j.colsurfa.2004.05.009
- [28] M.O. Abd El-Magied, S. Manar, B.Y. I., F.M. M., A.Z. M., M.M. and Rezk, Design of some ferrite-based nanoparticles for uranium removal from Sella leach liquor, International Journal of Environmental Analytical Chemistry, 1-27. DOI: 10.1080/03067319.2024.2429009
- [29] M.M. Rezk, A.S. Dhmees, M.O. Abd El-Magied, E.A. Manaa, H.S. El-Gendy, The influence of cobalt manganese ferrite nanoparticles (Co(0.5)Mn(0.5)Fe(2)O(4)) on reduction of hazardous effects of vanadate in adult rats, Toxicol Res (Camb), 9 (2020) 81-90. DOI: 10.1093/toxres/tfaa007
- [30] M.O. Abd El-Magied, M. Sopaih, R.A. Abdelhafez, Z.M. Anwar, Removal of arsenazo III dye from wastewater using some nano-engineered ferrite and magnetite adsorbents, Egyptian Journal of Chemistry, (2025) -. DOI: 10.21608/ejchem.2025.373841.11563
- [31] M.M. Ibrahim, H.S. El-Sheshtawy, M.O. Abd El-Magied, A.S. Dhmees, Mesoporous Al2O3 derived from blast furnace slag as a cost-effective adsorbent for U(VI) removal from aqueous solutions, International Journal of Environmental Analytical Chemistry, 103 (2021) 2948-2964. DOI: 10.1080/03067319.2021.1900150
- [32] W. Semida, A. Hassan, T.F. Mohammaden, S. Negm, M.O. Abd El-Magied, Utilizing green chemistry in the synthesis of modified chitosan biosorbents: application in La(III) ion recovery from the monazite leach liquor, Egyptian Journal of Chemistry, 0 (2023) 0-0. DOI: 10.21608/ejchem.2023.203780.7815
- [33] W.M. Semida, A.M. Hassan, T.F. Mohammaden, S.H. Negm, M.O.A. El-Magied, Microwave-assisted synthesis of functionalized chitosan adsorbents for cerium adsorption from aqueous Solutions, Radiochemistry, 65 (2023) 510-522. DOI: 10.1134/s1066362223040136
- [34] J. Coates, Interpretation of infrared spectra, A Practical Approach, in: Encyclopedia of Analytical Chemistry, 2000. DOI: 10.1002/9780470027318.a5606
- [35] M.O. Abd El-Magied, E.-S.A. Manaa, M.A.M. Youssef, M.N. Kouraim, A.S. Dhmees, E.M. Eldesouky, Uranium removal from aqueous medium using Co0.5Mn0.5Fe2O4 nanoparticles, Journal of Radioanalytical and Nuclear Chemistry, 327 (2021) 745-753. DOI: 10.1007/s10967-020-07571-1
- [36] A.N.A. Hosain, A. El Nemr, A. El Sikaily, M.E. Mahmoud, M.F. Amira, Surface modifications of nanochitosan coated magnetic nanoparticles and their applications in Pb(II), Cu(II) and Cd(II) removal, Journal of Environmental Chemical Engineering, 8 (2020) 104316. DOI: 10.1016/j.jece.2020.104316
- [37] R.R.d. Silva, L.C.d. Oliveira, G.V. Gabriel, J.I. Soletti, M.D. Bispo, S.S. Paulino, S.M. Meneghetti, G.C.d. Assis, A.P. Fernandes, W.G. Botero, Interaction of lead and calcium with biochar produced from cassava waste: perspectives for agricultural and environmental application, Journal of the Brazilian Chemical Society, 33 (2022) 1402-1413. DOI: 10.21577/0103-5053.20220076
- [38] X. Zhang, H. Fan, J. Yuan, J. Tian, Y. Wang, C. Lu, H. Han, W. Sun, The application and mechanism of iron sulfides in arsenic removal from water and wastewater: A critical review, Journal of Environmental Chemical Engineering, 10 (2022) 108856. DOI: 10.1016/j.jece.2022.108856
- [39] S. Alharthi, S.A. Alharthy, E.S.A. Manaa, M.O. Abd El-Magied, W.M. Salem, High adsorption performance of Cr(VI) ions from the electroplating waste solution using surface-modified porous poly 2-((methacryloxy)methyl)oxirane polymers, Zeitschrift für anorganische und allgemeine Chemie, 648 (2022) e202100327. DOI: 10.1002/zaac.202100327
- [40] J. Wang, X. Guo, Adsorption isotherm models: Classification, physical meaning, application and solving method, Chemosphere, 258 (2020) 127279. DOI: 10.1016/j.chemosphere.2020.127279
- [41] M.M. Ibrahim, H.S. El-Sheshtawy, M.O. Abd El-Magied, E.-S.A. Manaa, M.A.M. Youssef, M.N. Kouraim, E.M. Eldesouky, A.S. Dhmees, A facile and cost-effective adsorbent derived from industrial iron-making slag for uranium removal, Journal of Radioanalytical and Nuclear Chemistry, 329 (2021) 1291-1300. DOI: 10.1007/s10967-021-07914-6
- [42] S. Alharthi, M.O.A. El-Magied, Industrial by-product utilized synthesis of mesoporous aluminum silicate sorbent for thorium removal, Korean Journal of Chemical Engineering, 38 (2021) 2365-2374. DOI: 10.1007/s11814-021-0877-2
- [43] E.A. Matter, A.S. Dhmees, W.M. Salem, M.O.A. El-Magied, G.H.G. Ahmed, Extraction of rare earth elements from Monazite leach liquor using functionalized chitosan sorbents derived from shrimp waste, Environ Sci Pollut Res Int, 30 (2023) 108067-108084. DOI: 10.1007/s11356-023-29662-8
- [44] A.M. Abu El-Soad, G. Lazzara, M.O. Abd El-Magied, G. Cavallaro, J.S. Al-Otaibi, M.I. Sayyed, E.G. Kovaleva, Chitosan functionalized with carboxyl groups as a recyclable biomaterial for the adsorption of Cu (II) and Zn (II) ions in aqueous media, Int J Mol Sci, 23 (2022). DOI: 10.3390/ijms23042396

[45] J.S. Piccin, T.R.S.A. Cadaval, L.A.A. De Pinto, G.L. Dotto, Adsorption isotherms in liquid phase: experimental, modeling, and interpretations, Adsorption processes for water treatment and purification, (2017) 19-51. DOI: 10.1007/978-3-319-58136-1_2
[46] M.O. Abd El-Magied, M. Sopaih, Y.I. Bakr, M.M. Fawzy, Z.M. Anwar, M.M. Rezk, Design of some ferrite-based nanoparticles for

^[46] M.O. Abd El-Magied, M. Sopaih, Y.I. Bakr, M.M. Fawzy, Z.M. Anwar, M.M. Rezk, Design of some ferrite-based nanoparticles for uranium removal from Sella leach liquor, International Journal of Environmental Analytical Chemistry, (2024) 1-27. DOI: 10.1080/03067319.2024.2429009.